



Self-organized developmental patterning and differentiation in cerebral organoids

Magdalena Renner^{1,†}, Madeline A Lancaster^{1,2,†}, Shan Bian¹, Heejin Choi³ , Taeyun Ku³, Angela Peer¹, Kwanghun Chung^{3,4,5,6,7} & Juergen A Knoblich^{1,*} 

Abstract

Cerebral organoids recapitulate human brain development at a considerable level of detail, even in the absence of externally added signaling factors. The patterning events driving this self-organization are currently unknown. Here, we examine the developmental and differentiative capacity of cerebral organoids. Focusing on forebrain regions, we demonstrate the presence of a variety of discrete ventral and dorsal regions. Clearing and subsequent 3D reconstruction of entire organoids reveal that many of these regions are interconnected, suggesting that the entire range of dorso-ventral identities can be generated within continuous neuroepithelia. Consistent with this, we demonstrate the presence of forebrain organizing centers that express secreted growth factors, which may be involved in dorso-ventral patterning within organoids. Furthermore, we demonstrate the timed generation of neurons with mature morphologies, as well as the subsequent generation of astrocytes and oligodendrocytes. Our work provides the methodology and quality criteria for phenotypic analysis of brain organoids and shows that the spatial and temporal patterning events governing human brain development can be recapitulated *in vitro*.

Keywords development; human brain development; neurogenesis; organoid; patterning; signaling

Subject Categories Development & Differentiation

DOI 10.15252/embj.201694700 | Received 4 May 2016 | Revised 2 February 2017 | Accepted 9 February 2017 | Published online 10 March 2017

The EMBO Journal (2017) 36: 1316–1329

See also: **C Dias & F Guillemot** (May 2017)

Introduction

Our current understanding of mammalian brain development is largely derived from studies in animal models, particularly rodents. These studies have shed light on a variety of processes underlying brain patterning, neurogenesis, and neuronal positioning and maturation (Taverna *et al*, 2014). How these processes are conserved in humans and how they are modified to explain the enormous increase in size and complexity in the human brain, however, is much less clear (Lui *et al*, 2011; Geschwind & Rakic, 2013).

To overcome this problem and to model human neurodevelopmental disorders, multiple 3D culture systems have recently been developed that allow the recapitulation of human brain development *in vitro* starting from pluripotent stem cells (PSCs; Eiraku *et al*, 2008; Mariani *et al*, 2012; Kadoshima *et al*, 2013; Paşca *et al*, 2015). Such *in vitro* systems have great potential for revealing the human-specific aspects of formation of particular brain regions, but the extent to which these isolated brain regions model overall patterning is limited.

We have recently developed a 3D culture model termed cerebral organoids (Lancaster *et al*, 2013) that can recapitulate many aspects of brain development, including the establishment of discrete regions of the central nervous system (retina, forebrain, and choroid plexus), organized germinal zones, and both radial and tangential migration of cortical neuron populations. Unlike other protocols (Eiraku *et al*, 2008; Chambers *et al*, 2009; Kadoshima *et al*, 2013; Mariani *et al*, 2015; Paşca *et al*, 2015; Qian *et al*, 2016), cerebral organoids are not patterned by externally added growth factors or morphogens, suggesting that their development relies purely on self-organization.

In vivo, the developing forebrain is patterned by morphogen gradients secreted from organizing centers within the forebrain (Borello & Pierani, 2010). After neural tube closure, three main signaling centers determine forebrain anterior–posterior and dorsal–ventral patterning. Rostrally, the anterior neural ridge secretes Fgf8 family molecules. At the midline of the cortical hemispheres, the cortical hem secretes Wnts (Wnt2b, Wnt3a, Wnt5a) and Bmps (Bmp2, Bmp4, Bmp6, Bmp7). The cortical hem regulates dorsal–ventral

1 Institute of Molecular Biotechnology of the Austrian Academy of Sciences (IMBA), Vienna Biocenter (VBC), Vienna, Austria

2 MRC Laboratory of Molecular Biology, Cambridge Biomedical Campus, Cambridge, UK

3 Institute for Medical Engineering and Science, Massachusetts Institute of Technology (MIT), Cambridge, MA, USA

4 Picower Institute for Learning and Memory, MIT, Cambridge, MA, USA

5 Department of Chemical Engineering, MIT, Cambridge, MA, USA

6 Department of Brain and Cognitive Sciences, MIT, Cambridge, MA, USA

7 Broad Institute of Harvard University and MIT, Cambridge, MA, USA

*Corresponding author. Tel: +43 1 79044 4800; E-mail: juergen.knoblich@imba.oeaw.ac.at

†These authors contributed equally to this work

patterning of the cerebral cortex by promoting dorsal forebrain and repressing ventral forebrain identity (Caronia-Brown *et al*, 2014). Opposite to the hem, at the sharp boundary between dorsal and ventral telencephalon, the pallial–subpallial boundary (PSPB) or antihem separates dorsal from ventral forebrain. Cells at the PSPB express the soluble Wnt inhibitor Sfrp2, Fgf7, and the EGF-like factors, Tgf alpha, Nrg1, and Nrg3 (O’Leary *et al*, 2007; Medina & Abellán, 2009; Subramanian *et al*, 2009; Grove & Monuki, 2013).

Following establishment of these key morphogenetic boundaries, neural progenitors begin to generate neurons of specific identities following a precise temporal program (Molyneaux *et al*, 2007). The first neurons to populate the dorsal cortex are the Cajal–Retzius cells, which are generated in regions adjacent to the cortex including hem and PSPB and then migrate into the early preplate of the cortex. Subsequently, neurons are generated from radial glia in an inside-out manner with deep-layer identities being generated early, and superficial identities being generated later. Finally, forebrain neural stem cells terminate their divisions by producing glial identities including astrocytes and oligodendrocytes. While this pattern of development is highly stereotypical across mammals, the extent to which these spatial and temporal patterning events can be recapitulated *in vitro* is currently unknown.

In contrast to actual organs, organoids lack externally recognizable body axes that guide their gross morphogenesis and help with phenotypic analysis. Therefore, cerebral organoids require careful analysis to decipher regional identities and spatial organization. Here, we systematically analyze regional identity in cerebral organoids using established markers to reveal discrete dorsal and ventral forebrain regions. We show that variability within organoid cultures can be addressed by using a critical marker set during the analysis of development. This approach, along with clearing of organoids to determine the overall 3D arrangement, reveals that major forebrain signaling centers are present within organoids and neuronal and glial differentiation occurs in a timed manner matching that seen *in vivo*.

Results

Forebrain regional specification in cerebral organoids

Cerebral organoids form complex tissues of variable identities. However, because tissues appear somewhat randomly distributed throughout the organoids, and without body axes as a neuroanatomical guide, it can be difficult to unambiguously identify specific brain regions. We therefore researched numerous markers of brain regional identity and cross-checked them for consistency between mouse and human brain development (Eurexpress and BrainSpan; Geffers *et al*, 2012; Miller *et al*, 2014). *In vivo*, the forebrain is subdivided into various distinct regions that assume stereotypic positions along the dorso-ventral (D/V) and medio-lateral axes (Sanes *et al*, 2011). The choroid plexus forms at the most medial–dorsal site, followed by the developing hippocampus and dorsal cortex. Laterally, the cortex abuts the ventral forebrain that comprises the ganglionic eminences (GE) during embryonic development. The GE is the major source of cortical interneurons. It is subdivided into medial, lateral, and caudal ganglionic eminences (LGE, MGE, CGE) that can be distinguished by marker expression and morphology (Hansen *et al*, 2013; Ma *et al*, 2013). We

ascertained a set of markers that are specific for these subregions and were used for subsequent analyses either in isolation or in combination with other markers (summarized in Fig 1A).

A hallmark of the cerebral organoid approach is the formation of large continuous forebrain tissues (here defined as radially organized tissues greater than 400 μm in diameter) containing well-defined progenitor zones and neuronal populations. Our analysis was restricted to those regions as they are structurally more similar to the developing human brain and better defined than small neural rosettes that can also form within cerebral organoids. To determine the D/V identity of the forebrain tissues (forebrain identity was confirmed by staining for FOXG1: Fig EV1), we performed a series of immunohistochemical stainings. We stained for PAX6, widely considered a dorsal cortical marker (Georgala *et al*, 2011; Shi *et al*, 2012) and the more definitive dorsal forebrain marker TBR2. PAX6 is expressed in radial glial progenitors in the ventricular zone (VZ), and these radial glia give rise to intermediate progenitor cells, which downregulate PAX6, express TBR2, and move to the subventricular zone (SVZ; Englund, 2005). Besides regions with cortical morphology containing both PAX6- and TBR2-positive cells in the typical VZ–SVZ arrangement (Fig 1B; Lancaster *et al*, 2013), we detected many PAX6-positive but TBR2-negative tissues with typical radial VZ organization (Fig 1D). Although these regions were morphologically indistinguishable from dorsal forebrain, subsequent staining for GSX2 confirmed their ventral GE identity, more specifically LGE or CGE (Fig 1D and E). Notably, when separate GSX2⁺ and TBR2⁺ regions were present within a single organoid, PAX6 staining revealed a lower level of expression in GSX2⁺ regions, consistent with the *in vivo* pattern (Georgala *et al*, 2011). However, in organoids without TBR2⁺ dorsal regions with high PAX6 as a reference, PAX6 staining alone or in combination with morphology is not sufficient to assign dorsal cortex identity in brain organoid models. Thus, cerebral organoids contain both dorsal and ventral forebrain regions with organized progenitor zones and regional identity needs to be confirmed by careful marker stainings.

To further characterize the GSX2-positive GE regions, we used the MGE marker NKX2.1. NKX2.1 staining in radially organized tissues was very rare and overlapped with GSX2 where it probably marked the transition from LGE to MGE, a pattern also seen *in vivo* (Fig 1F). *In vivo*, the GE generates interneurons that migrate tangentially into the dorsal forebrain (Hansen *et al*, 2013; Ma *et al*, 2013). Indeed, GE regions in organoids not only contained abundant DLX2-positive intermediate progenitors and young neurons (Fig 1G), but were also surrounded by abundant VGAT-positive GABAergic interneurons (Fig 1H). Consistent with previous observations (Lancaster *et al*, 2013), interneurons were also found in dorsal forebrain regions (Fig 1I, arrows) in the majority of organoids containing dorsal regions (Table EV1). However, in two organoids of almost exclusively dorsal identity, we did not find interneurons, which could be due to the absence of a ventral region. Thus, the interaction of regions with different cortical identities is preserved in organoid models.

In addition to ventral GE, cerebral organoids also contained the medial parts of the dorsal forebrain, the choroid plexus, and in rare cases hippocampus (Lancaster *et al*, 2013). Choroid plexus (CP) stained positive for the CP marker TTR (Fig 1J). Live imaging of choroid plexus tissue revealed small unidirectionally moving particles, indicating that circulation of the surrounding liquid by CP cilia is preserved in organoids (Fig EV1 and Movie EV1). Hippocampal

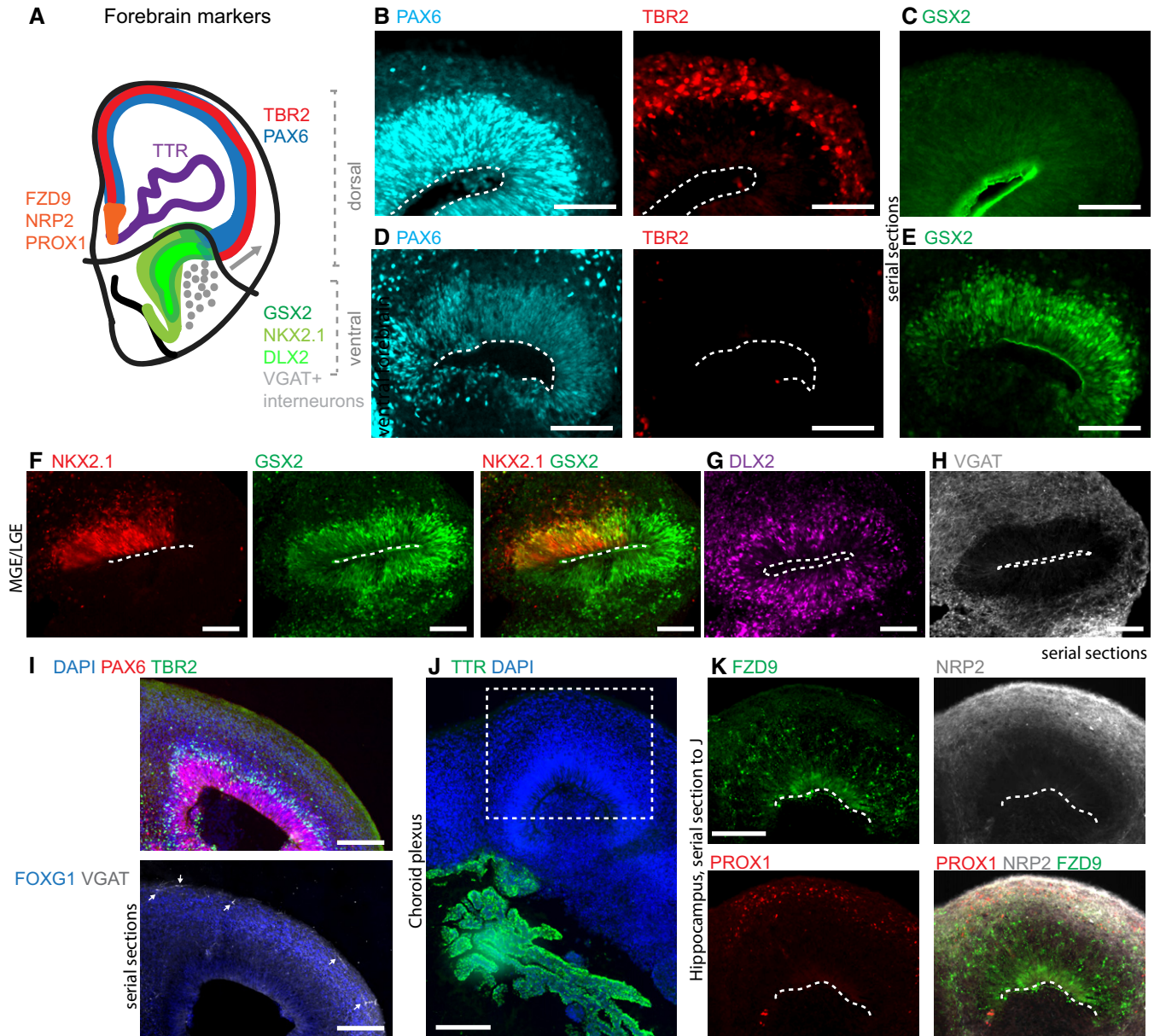


Figure 1. Cerebral organoids organize into different forebrain regions.

A Summary of the markers used for forebrain regional characterization.
 B, C Dorsal forebrain regions stain (B) positive for PAX6 (cyan, radial glia progenitors in the VZ) and TBR2 (red, intermediate progenitors in the SVZ) and (C) negative for GSX2 (green). GSX2 staining along the ventricle is unspecific signal, and panel (C) shows a serial section to (B).
 D, E LGE/CGE regions can be (D) PAX6 positive (cyan) and are TBR2 negative (red), (E) but are positive for GSX2 (green). Panel (E) shows a serial section to (D).
 F–H (F) MGE stains for NKX2.1 (red) and can be found continuous with LGE/CGE positive for GSX2 (green). Radially organized NKX2.1 is very rare. (G) Progenitors and young neurons of the GE stain for DLX2 (magenta). (H) VGAT interneurons (white) are densely arranged around GE regions. Panels (G) and (H) are serial sections to (F).
 I VGAT-positive interneurons (white arrows) can be found in dorsal forebrain tissue marked by TBR2-positive cells (green) in the SVZ. Shown are serial sections.
 J, K (J) TTR (green) stains choroid plexus. (K) Expression of hippocampal markers adjacent to choroid plexus. Panel (K) shows a serial section to (J), and the boxed area in (J) is analyzed. Note that fully differentiated hippocampal tissue expressing all three markers was relatively rare.
 Data information: Quantifications of all stainings are summarized in Table EV1. FOXG1 staining to confirm forebrain identity for all regions is shown in Fig EV1. Scale bars: 100 μm (B–H), 200 μm (I–K). Dashed lines indicate apical/ventricular surface.

tissues stained positive for the dorsal forebrain markers PAX6 and TBR2 (Fig EV1) and the hippocampal markers PROX1, FZD9, and NRP2 (Fig 1K). Thus, both lateral and medial cortical tissues can be uniquely identified in organoids.

Efficiency of generation of forebrain regions

To address the degree of variability in regional identity determination, we quantified dorsal or non-dorsal identity of large forebrain

Figure 2. Organization of large regions within cerebral organoids.

- A Selection of organoids for analysis is based on large, radially organized tissues (arrows) as seen by DAPI staining on entire slides scanned by a fluorescence slide scanner. Rosette-like structures (x) were disregarded. Arrows point at dorsal forebrain structures > 400 μm in diameter. The arrowhead marks a non-forebrain structure (Fig EV1). Serial sections 200 μm apart through the entire organoids were analyzed. Each section contained two to six individual organoids that were used for analysis if at least one organoid contained radially organized tissue that was > 400 μm in diameter.
- B Staining of organoids with PAX6 (green, RG in SVZ) and TBR2 (red, IP of dorsal forebrain in SVZ) to identify dorsal forebrain regions > 400 μm .
- C Higher magnification image of tissue marked in (B) showing PAX6 and TBR2 staining.
- D Quantification of experiments showing the percentage of organoids per experiment that contained dorsal forebrain regions > 400 μm , large radial tissue of non-dorsal identity > 400 μm , or no large radial tissues > 400 μm . For each experiment, three to 11 organoids were analyzed at one or more time points between 30 and 70 days, and each bar represents an experiment. Organoids of all ages (30–70 days) were capable of efficiently generating dorsal forebrain tissue.
- E Optical sections of an organoid cleared by SWITCH and stained by 4',6-diamidino-2-phenylindole (DAPI). Examples of individual ventricular zones belonging to one structure are marked in different colors. Arrowheads point to choroid plexus (arrow) attached to the organoid throughout multiple optical sections.
- F The ventricular system of organoids, cleared by SWITCH and imaged entirely in 3D, was reconstructed by manually outlining the ventricular zone by a line in the program "Amira" every 9–10 μm through the entire stack. Example of one plane with the 3D rendered ventricular system in purple. Movie EV2 shows entire reconstruction. Arrowheads and arrow as in (E).
- G 3D reconstruction of an entire organoid, arrow points to choroid plexus, arrowheads as in (E).
- Data information: Scale bars: 500 μm (A, B), 200 μm (C).

regions in 104 organoids from 22 distinct experiments. For this, we generated 20- μm sections spanning the entire volume of each organoid in 200- μm intervals. Only tissues containing radially organized regions of more than 400 μm end-to-end diameter were analyzed (Fig 2A arrows; smaller rosettes, marked with "x", were disregarded; FOXG1 staining was used to determine forebrain identity, Fig EV1). Importantly, we only processed organoids that passed the quality criteria previously described (Lancaster & Knoblich, 2014), namely clearing of EB borders before transfer to neural induction medium, formation of radially organized neuroepithelium in neural induction medium before Matrigel embedding, and outgrowth and development of defined buds in Matrigel without massive cyst formation and/or complete overgrowth by migratory cells.

We imaged the entire volume of each organoid by an automated slide scanner and identified dorsal forebrain as tissue containing a radially organized VZ and staining positive for both PAX6 and TBR2, or FOXG1 and TBR2 (Fig 2B and C). We found large dorsal forebrain tissues in 16 out of 22 experiments (Fig 2D). Of these, 12 experiments displayed large dorsal regions to varying degrees, while four experiments contained dorsal forebrain tissues larger than 400 μm in all the organoids analyzed. In the six experiments where we could not find any tissues with large dorsal forebrain, the organoids either generated large radially organized regions with overall low efficiency or the tissue was of ventral, non-dorsal, or unknown identity (Fig 2D).

Organoid clearing and 3D imaging reveal tissue interconnectivity

To visualize entire organoids in 3D, we used the recently described SWITCH protocol (Murray *et al*, 2015) that allows clearing and imaging of highly diffractive brain tissue. This enabled an unprecedented representation of organoid structure, revealing a high level of internal tissue connectivity. Most importantly, this experiment demonstrated that many of the cortical tissues that appeared isolated in 2D sections were instead part of one large heavily intertwined cortical region as they were connected only a few optical sections later (Fig 2E). We therefore marked all ventricles throughout the entire organoid and performed 3D reconstruction, revealing a complex three-dimensional ventricular network within the organoid (Fig 2F and G, and Movie EV2).

These findings suggest that tissues of different dorsal–ventral forebrain identities might be connected in a single neuroepithelial structure within organoids. This structural organization may allow not only for short-distance signaling between forebrain regions, but also long-distance communication through signaling molecules secreted into the connected ventricular network. The presence of an elaborate CP (Fig 2E and F, arrow) attached to large, radially organized tissues (Fig 2E and F, arrowheads), and our findings that the CP generated unidirectional flow (Fig EV1 and Movie EV1), supports this hypothesis.

Cerebral organoids generate forebrain organizing centers

In vivo, the dorsal forebrain is patterned along the dorsal–ventral axis by two organizing centers: the cortical hem located medially between the choroid plexus and cortex, and the PSPB or antihem, separating the cortex from the lateral GE. To address whether organoids contain forebrain organizing centers that could influence the generation of dorsal and ventral forebrain regions, we performed immunohistochemistry to identify regions reminiscent of the cortical hem and the PSPB. To identify PSPB structures, we analyzed the same set of organoids as in Fig 2D. We identified the PSPB as dorsal forebrain tissue (PAX6⁺, TBR2⁺, GSX2⁻) directly abutting ventral forebrain tissue (GSX2⁺, PAX6^{+/-}, TBR2⁻; Fig 3A). Indeed in seven out of 22 experiments, we found several tissues with a sharp boundary between dorsal and ventral forebrain tissues (Fig 3A and B). This staining is consistent with the arrangement of a PSPB (Fig 3C).

To identify hem in cerebral organoids, we performed immunohistological experiments using markers for specific brain regions. To exclude artifacts from mispatterned organoids, we included only those experiments in which more than 50% of all organoids contained dorsal forebrain tissue larger than 400 μm in diameter. Sections adjacent to those large dorsal forebrain regions were stained for PAX6, LMX1a (Chizhikov *et al*, 2010), and the choroid plexus marker TTR. Indeed, in nine experiments analyzed (53 organoids in total, Table EV1), we detected LMX1a-positive cell populations between the choroid plexus and the dorsal forebrain in several organoids, recapitulating the organization of the cortical hem (Fig 3D and E). This might be an underestimate as organoids do not display an externally visible axis and therefore some hem structures

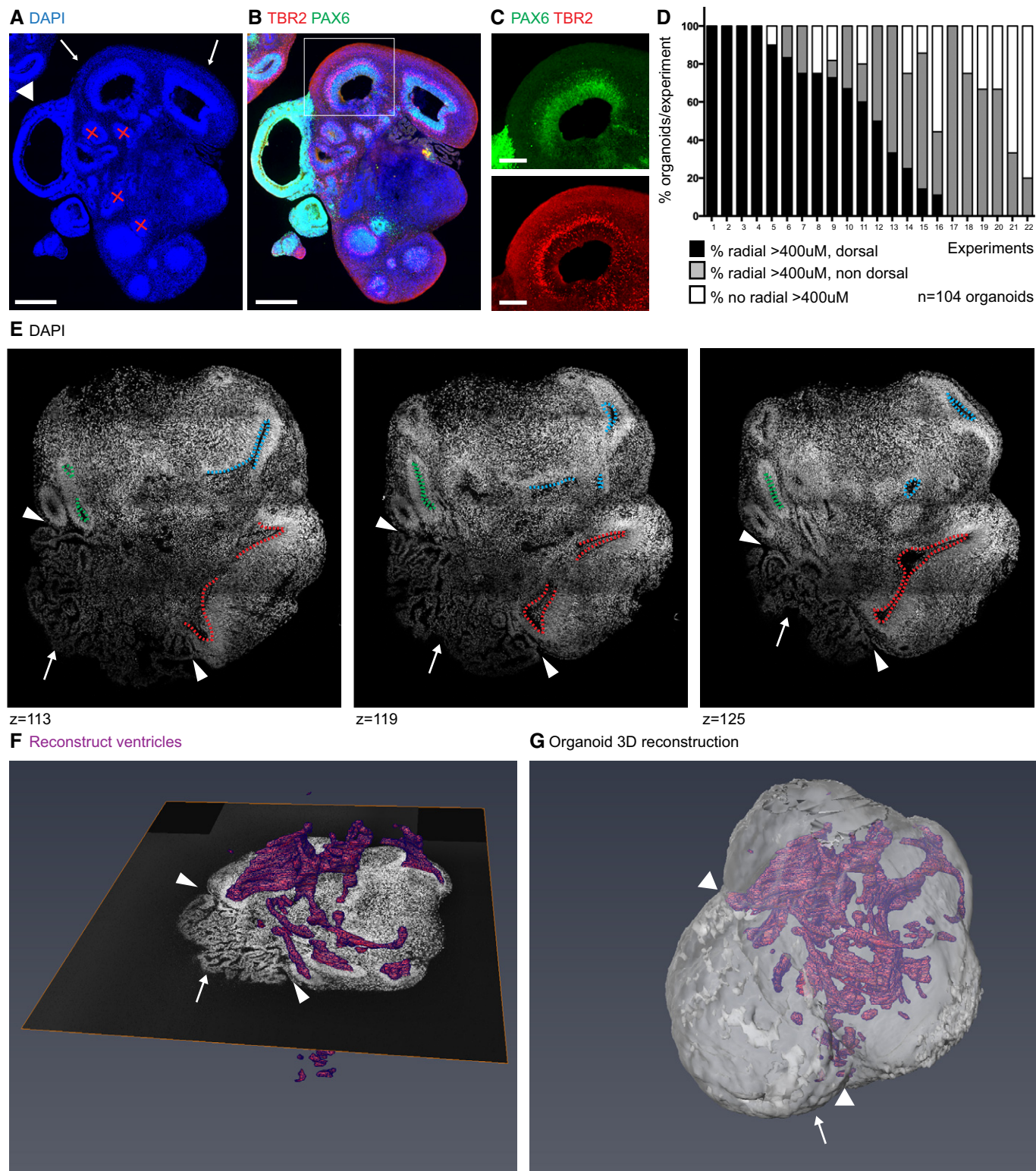


Figure 2.

could be missed in the random 2D sections through complex 3D tissues. When we analyzed the presence of a PSPB in the experiments that were analyzed for cortical hem, we found that 11 out of 53 organoids contained both hem and PSPB tissues. Twenty-one

contained only hem and nine contained only PSPB, while the remaining 12 organoids contained neither hem nor PSPB (Fig 3F). These results suggest that organoids are capable of generating structures reminiscent of forebrain organizing centers.

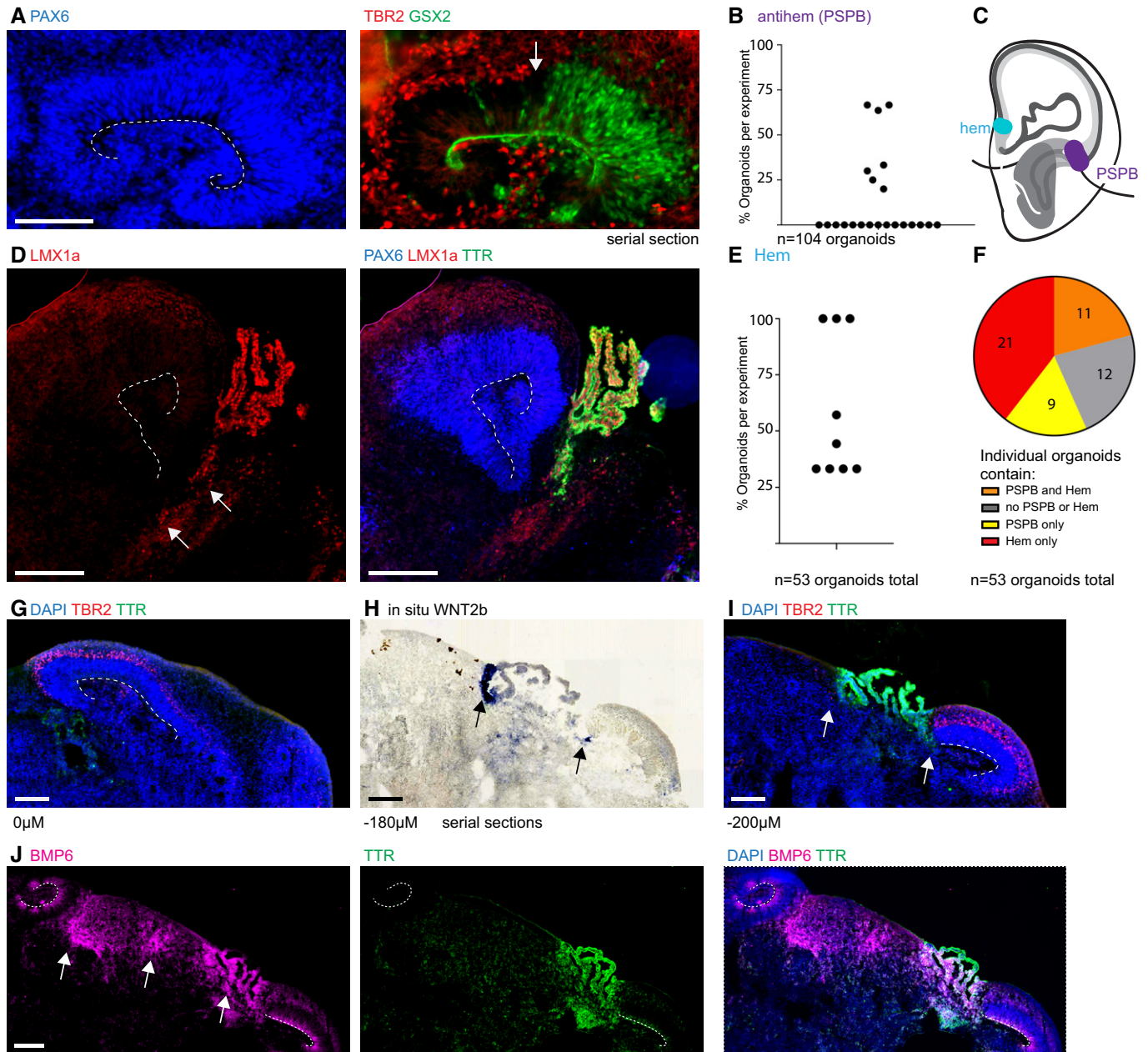


Figure 3. Cerebral organoids contain tissue reminiscent of forebrain organizing centers.

- A Tissue arrangement is reminiscent of the pallial–subpallial boundary (PSPB)/anterior hem with an abrupt termination of TBR2 staining (red) where GSX2 staining (green) begins (arrow). The whole tissue is positive for PAX6 (blue) on the adjacent section.
- B Quantification of the percentage of organoids within individual experiments that contained tissues reminiscent of a PSPB; the same organoid dataset as in Fig 2D was analyzed.
- C Schematic depiction of the organizing centers hem and PSPB within the forebrain.
- D Tissues containing LMX1a staining (red, arrows) can be found in between choroid plexus (TTR, green) and dorsal forebrain (PAX6 positive, blue). The presence of TBR2 was verified on an adjacent section. LMX1a also stains the choroid plexus.
- E Quantification of the percentage of organoids within individual experiments containing hem-like tissue as described in (D). Only experiments containing large dorsal forebrain regions in > 50% of organoids were analyzed.
- F Fifty-three organoids analyzed in (E) were analyzed also for the presence of PSPB-like tissue on adjacent sections.
- G–I TBR2 staining (magenta) for dorsal forebrain and TTR staining (green) for choroid plexus on serial sections across 200 μ m and *in situ* hybridization for Wnt2b which is specifically expressed in the cortical hem (arrows). Note the presence of dorsal cortical tissue (G, I) flanking the Wnt2b hem with choroid plexus in between. Z-positions are indicated.
- J BMP6 (magenta) is expressed in the hem and choroid plexus (arrows). A serial section to (G–I) is shown.

Data information: Quantifications are summarized in Table EV1. Scale bars: 100 μ m (A), 200 μ m (D, G–J).

The cortical hem has an important signaling function within the dorsal forebrain. The signaling factor *Wnt2b* is expressed in a narrow stripe, while other signaling molecules such as *Wnt3a*, *Bmp6*, and *Bmp7* are more dispersed (Grove *et al*, 1998; Abu-Khalil *et al*, 2004). Indeed, using *in situ* hybridization on serial sections, we found that *Wnt2b* was expressed in organoids between the choroid plexus and the dorsal forebrain (Fig 3G–I, arrows). For quantification, we used anti-BMP6 staining to be compatible with immunohistological identification of regional markers. We analyzed BMP6 expression in experiments in which we could find dorsal forebrain tissue larger than 400 μm in diameter in more than 50% of organoids. BMP6 is expressed in the cortical hem and also choroid plexus. We analyzed 29 organoids from five independent experiments and found BMP6-positive hem tissue located next to dorsal forebrain tissue in 79% of them. All of these regions were also positive for *LMX1a* in serial sections (Fig EV2).

Thus, cerebral organoids contain the organizing centers that are involved in patterning the mammalian brain *in vivo*. Our analysis shows that they can produce signaling molecules normally present in those organizers. These morphogens might influence regional identity both in the immediate vicinity, but also over long distances through the interconnected ventricular network, although genetic loss-of-function analysis will be required to demonstrate that cortical patterning in organoids is indeed influenced by the presence of PSPB or hem tissue.

Timed generation of excitatory neuronal subtypes

Having observed the presence of spatial patterning, we next sought to test whether brain organoids displayed evidence of temporal patterning. The developing dorsal cortex *in vivo* displays remarkable timing in the generation of the various neuron types that make up the six layers of the cortex (Rakic, 1974; Hevner *et al*, 2003; Molyneaux *et al*, 2007; Gaspard *et al*, 2008). Specifically, Cajal–Retzius cells are generated first in regions adjacent to the cortex, followed by the sequential generation of deep-layer neurons and then superficial layer neurons. Therefore, we examined whether cerebral organoids displayed a similar timed generation of these excitatory neuron types. We performed staining for the marker of Cajal–Retzius cells, *Reelin*, which displayed an abundance of staining in early organoids (day 42) soon after the initiation of neurogenesis followed by a gradual decrease in abundance over time (Fig 4A). Staining for the deep-layer marker *CTIP2* and the superficial layer marker *SATB2* at various time points revealed abundant *CTIP2* cells at day 48, whereas *SATB2* neurons were largely absent at this time point, instead appearing around day 66 and increasing until day 102 (Fig 4B). We further tested for the presence of cells with a glial identity, which are believed to be generated lastly from the terminal divisions of neural stem cells (Sauvageot, 2002). GFAP staining revealed cells with strong positivity and astrocytic morphology beginning at approximately 100 days (Fig 4C). Thus, the relative emergence of cell types matches that observed *in vivo* where *Reelin*-positive cells are generated first, followed by deep-layer *CTIP2*-positive cells, then *SATB2*-positive superficial layer neurons, and finally cells with glial identities.

To further characterize this putative temporal patterning, we quantified the relative abundance of *Reelin*⁺, *CTIP2*⁺, or *SATB2*⁺ neurons, and of GFAP⁺ cells with astrocytic morphology. We

quantified organoids from 15 separate experiments ranging from 33 to 160 days in culture, with at least four organoids per time point (quantification summarized in Table EV2). This revealed the highest abundance of *Reelin* cells during the earliest time points, followed by a peak of *CTIP2*⁺ cells, then *SATB2*⁺ neurons, and finally GFAP⁺ astrocytes (Fig 4D). Finally, we examined the robustness of astrocyte generation by quantifying the number of astrocyte-containing organoids at each time point. We found that this fraction increased with time until finally by approximately 140 days all of the organoids analyzed displayed at least some astrocytes (Fig 4E).

Neurons and glia adopt mature morphological features

We next examined the morphology of excitatory neurons to establish whether they displayed typical morphological characteristics of dorsal cortical excitatory neurons, which are also termed pyramidal cells due to their triangular cell shape and their primary dendrite (Elston, 2003). We performed staining for the markers *SATB2* and *CTIP2* in combination with the dendritic marker *MAP2*. Numerous neurons of the dorsal cortical region displayed thickened dendrites extending radially outward, much like the primary dendrite typical of pyramidal cells (Fig 5A). Numerous outer branching dendrites could also be seen, reminiscent of so-called apical tufts. Imaris tracing of dendrites on a region with sparse staining identified individual dendritic trees, showing the presence of a primary dendrite and distal branching (Fig 5B). Furthermore, sparse labeling by electroporation with a membrane targeting GFP construct revealed neurons with thick primary dendrite and extensive distal branching (Fig 5C). These data suggest excitatory neurons in cerebral organoids are able to mature and take on the typical morphology seen *in vivo*.

We further characterized the cells of glial identities by staining for the broad glial marker GFAP as well as the glutamate transporter *GLT1* which is expressed in astrocytes. Astrocytes were positive for both markers and displayed typical morphology consisting of numerous elongated processes (Fig 5D). Furthermore, *O4* staining revealed the presence of oligodendrocytes, which primarily resided in the central regions of the organoid, where cells were sparse (Fig 5E). In addition, cells with *OLIG1* staining could be identified consistent with oligodendrocyte identity (Fig 5F). Costaining for *CTIP2* and *MAP2* revealed a close association of GFAP-positive astrocytes and differentiated cortical neurons (Fig 5G). Interestingly, in addition to astrocytes and oligodendrocytes with typical morphology, we also observed highly positive GFAP cells lining the outer surface of the brain organoids (Fig 5H). Finally, very old organoids (day 229) were almost entirely populated by glia showing staining for both GFAP and *GLT1* (Fig 5I). Thus, our data indicate that cerebral organoids can model the emergence and morphological differentiation of glial cells.

Discussion

Our findings demonstrate the remarkable ability of cerebral organoids to self-organize through endogenous patterning events that mimic the developing brain *in vivo*. Using detailed marker analysis, we have shown that cerebral organoids can form distinct forebrain structures, and we describe the variability and efficiency of generation of these regions. Furthermore, we identified tissues reminiscent

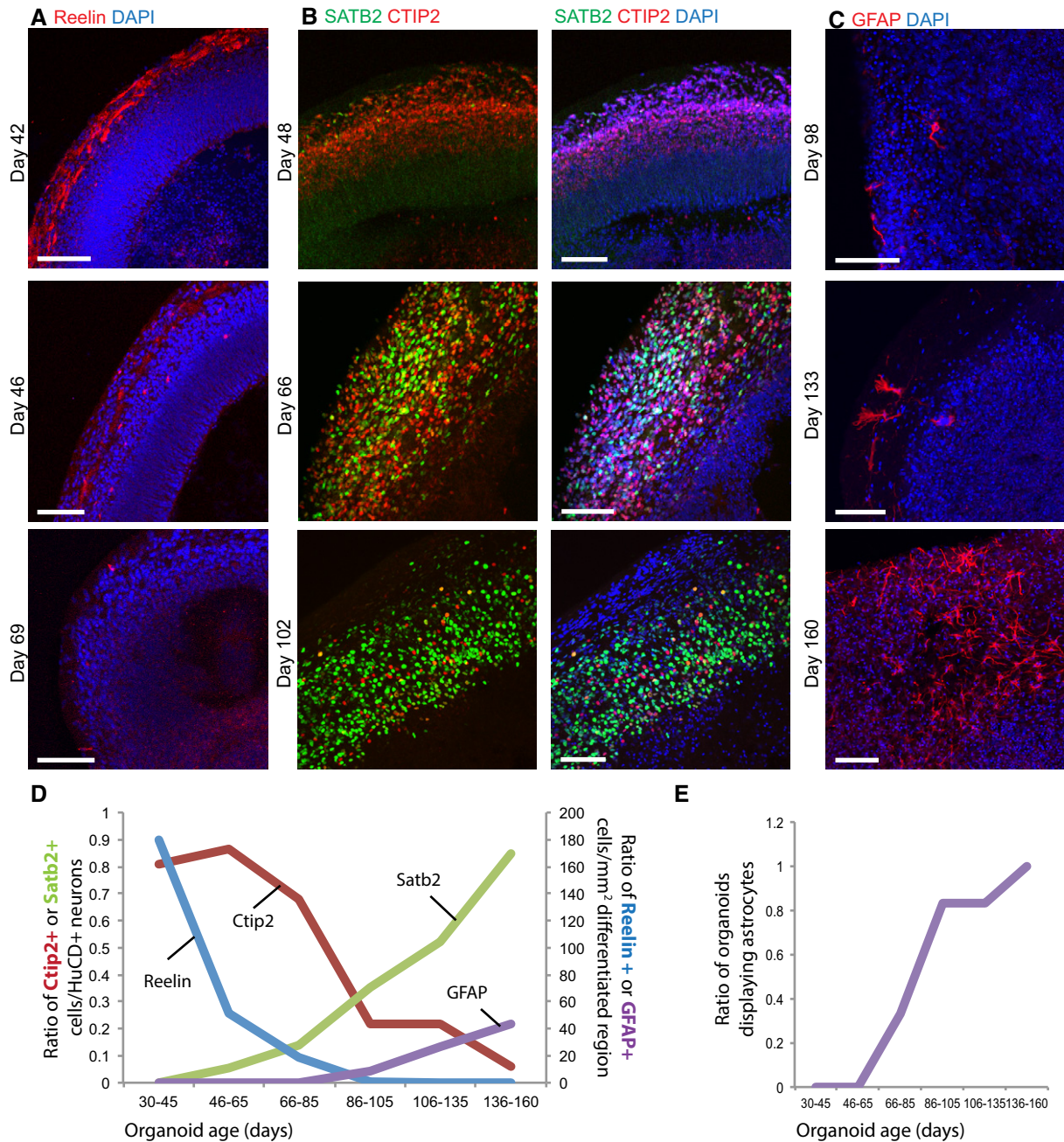


Figure 4. Temporal patterning of dorsal forebrain is recapitulated in cerebral organoids.

- A Staining for early-born Cajal–Retzius cells with the marker Reelin (red) shows strong staining at day 42 with decreasing staining at day 46 and day 69.
- B Staining for markers of deep-layer early-born neurons (CTIP2, red) and upper layer late-born neurons (SATB2, green) reveals progressive switching from CTIP2⁺ neuron production to SATB2⁺ neuron production.
- C Staining for GFAP (red) reveals cells with typical astrocyte morphology at day 98 and increasing in abundance over time.
- D Quantification of neuron and glial identities over time. CTIP2 and SATB2 were counted as a ratio of HuC/D⁺ neurons (left y-axis). Because both Reelin and GFAP are not nuclear markers, these were instead quantified as cell counts per mm² of differentiated region (intermediate zone/cortical plate, excluding germinal zones) as defined by DCX staining (right y-axis). Measurements were binned into six time windows spanning day 30 to day 160. 15 independent experiments were quantified with at least four organoids from at least two experiments per time window.
- E Quantification of the number of organoids displaying at least some GFAP⁺ astrocytes. Samples were the same as for panel (D).

Data information: Quantifications are summarized in Table EV2. Scale bars in all panels are 100 μ m.

of the cortical hem and PSPB, which *in vivo* have vital functions in forebrain patterning. In support of this finding, a recent single-cell transcriptome study also identified cells expressing hem-specific

genes in cerebral organoids (Camp *et al*, 2015). Although these tissues resembling organizing centers are formed in cerebral organoids, it remains to be determined whether they play a direct

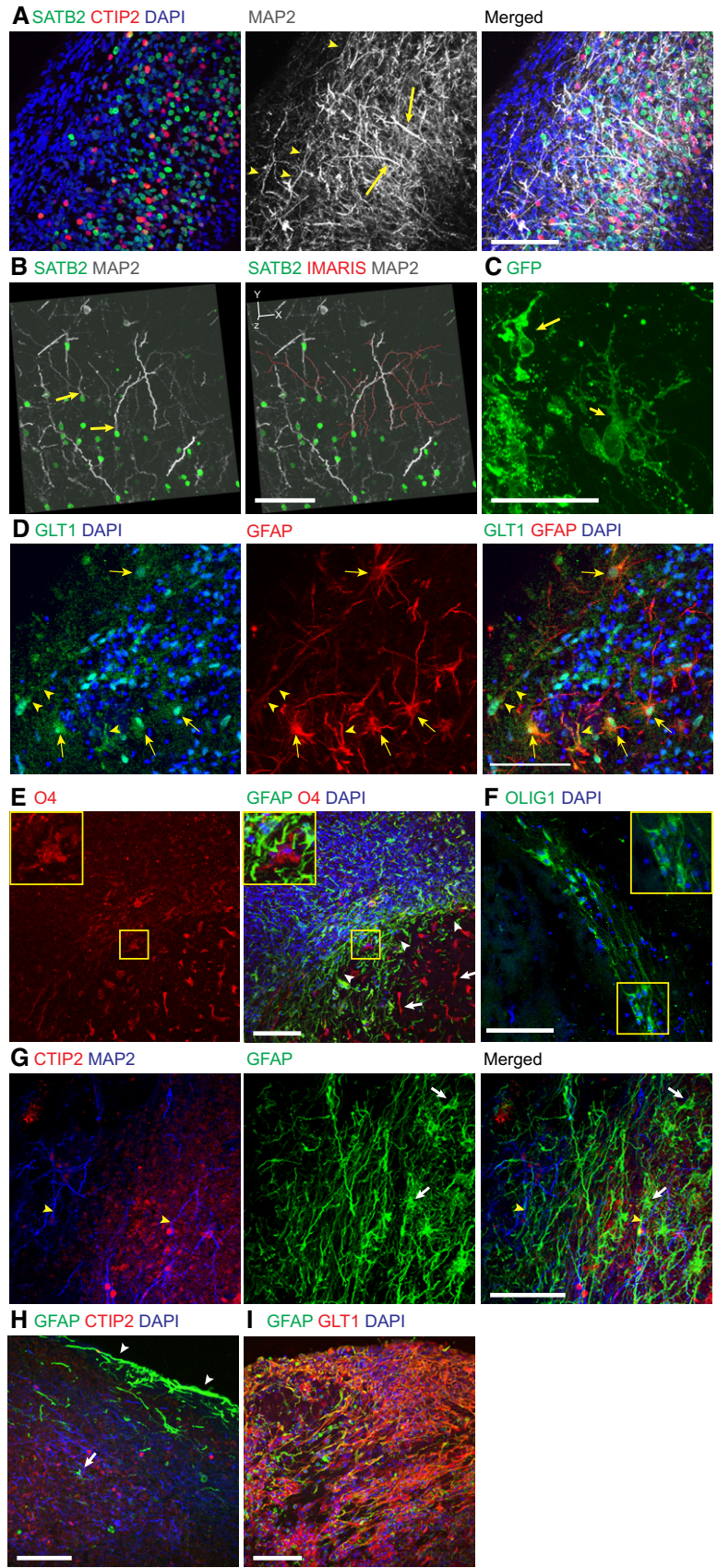


Figure 5.

Figure 5. Maturation of neuronal morphology and glial identities in cerebral organoids.

- A Staining for neuronal morphology with the dendrite marker MAP2 (grey) and cortical neuronal markers CTIP2 (red) and SATB2 (green), revealing large radially oriented dendrites (arrows) with perpendicular branching along the basal surface (arrowheads).
- B 3D reconstruction based on Z-stacks (axes shown in upper left) and IMARIS tracing (red) of dendrite trees of individual SATB2⁺ neurons, revealing a primary dendrite (arrows) with multiple branches, typical of pyramidal neuron morphology.
- C Neurons marked by an electroporated construct encoding farnesylated GFP targeted to the membrane in order to visualize cell morphology reveal cells with a major dendrite (arrows) proximal to the cell body and more distal branching, consistent with pyramidal cell morphology.
- D Staining at day 142 for astrocytes using the broad marker GFAP (red) and the astrocyte marker GLT1 (green). Note the numerous cells with typical astrocyte morphology and exhibiting nuclear/diffuse cytosolic GLT1 staining (arrows) as well as some staining in processes (arrowheads).
- E Staining for the oligodendrocyte marker O4 (red) reveals numerous O4⁺ cells on the interior of the organoid (arrows) in a cell sparse zone, whereas numerous nuclei (DAPI, blue) and astrocytes are located more externally (arrowheads). Inset shows higher magnification of an O4⁺ cell.
- F Staining for the marker OLIG1 additionally marks oligodendrocytes located in a stream in the interior of the organoid. Inset shows a higher magnification of several OLIG1⁺ cells.
- G Costaining for neuronal markers CTIP2 (red) and the dendrite marker MAP2 (blue) as well as GFAP (green) reveals astrocytes (arrows) and astrocytic processes in close proximity to neuronal dendrites (blue, arrowheads).
- H Highly GFAP⁺ (green) thick processes (arrowheads) can cover the surface of the organoids, whereas astrocytes with typical morphology can be seen more internally (arrow).
- I Costaining for GFAP (green) and GLT1 (red) in a much older organoid (229 days) reveals extensive overgrowth of glia at this late time point.
- Data information: Scale bars: 50 μ m (C), 100 μ m in all remaining panels.

functional role in organoid patterning. Unlike the hem, the antihem has not been proven to be an organizing center *in vivo*; however, its absence leads to a severe disruption of the radial glia progenitor palisade at the PSPB, raising a strong parallel with the function of the hem in organizing the hippocampal radial glia progenitor cells (Subramanian *et al.*, 2009).

Interestingly, our study revealed substantial variability among organoid experiments in the efficiency of generating dorsal or ventral forebrain tissue as well as other tissues whose identity we have not discerned. One hypothesis is that this variability arises depending on which organizing centers are formed. However, resolving the relationship between the presence of organizing centers and regional identity is highly challenging, since by definition, dorsal forebrain is found next to all identified hem tissues and dorsal forebrain and ventral forebrain are always curtailing the PSPB. Furthermore, organizing centers may be active only at certain developmental stages of individual organoids and might not be visible during the entire organoid life span, making it difficult to unambiguously discern which patterning cues are/have been present. Nonetheless, the fact that we observe formation of various different, organized tissue identities within the same organoid without providing external signaling molecules suggests that intrinsic signaling processes and patterning are at work during organoid development. Future functional studies and manipulations will be required to test whether these regions consistent with organizing centers are indeed involved in intrinsic patterning of cerebral organoids.

Making organoids transparent by the recently described SWITCH method (Murray *et al.*, 2015) and imaging of the entire structure allowed us to overcome some of the limitations of analysis of 3D organoids by 2D sections. Our results revealed a significant degree of tissue interconnectivity, even though the abundance of internal connections of the ventricular system varied across different organoids. The internal connection of organoids via a ventricular system has important implications for how we perceive tissue interactions in 3D. Signaling molecules could travel throughout the organoid, and tissues that are seemingly separated by long distances based on histological sections could actually be physically connected and influence each other.

These results underline the remarkable capacity of pluripotent stem cell-derived brain tissues to form various forebrain structures solely by self-organization. This shows that even the highly complex development of the telencephalon can be carried out to a surprisingly large extent without external signaling cues. Other published protocols for 3D brain tissue rely on the addition of signaling molecules to drive induction of defined tissue identities (Eiraku *et al.*, 2008; Chambers *et al.*, 2009; Kadoshima *et al.*, 2013; Mariani *et al.*, 2015; Paşca *et al.*, 2015; Qian *et al.*, 2016). This leads to the formation of homogeneous tissue that lacks crucial interactions of different brain regions such as the spatial integration of GABAergic interneurons with excitatory dorsal forebrain neurons. Furthermore, this may explain the capacity for whole brain organoids to form larger, more continuous cortical tissues, due to the interconnectivity with other forebrain regions such as cortical hem, which is important for cortical expansion *in vivo* (Caronia-Brown *et al.*, 2014) or CP, which *in vivo* generates ventricular cerebral spinal fluid.

Our findings reveal that not only are cerebral organoids capable of intrinsic spatial patterning, but they also display acquisition of cell identity in a timed manner that closely mimics the temporal patterning seen *in vivo* with sequential waves of neurons expressing Reelin, CTIP2, and SATB2. While the timing seen in organoids is overall somewhat slower than that described for 2D cultures (Gaspard *et al.*, 2008), it is closer to that seen *in vivo* for the developing human brain (<http://developinghumanbrain.org>). Importantly, while some subtle separation of deep and superficial neurons can be seen in organoids, overall they do not display the separation into discrete layers as would be seen *in vivo*. This may be due to a lack of later spatial organization into the cortical plate, a prerequisite of cortical layer formation. Finally, the timed formation of glia further demonstrates the potential utility of organoids as a route to study these supportive non-neural types and may even indicate a potential for myelination.

Although these findings identify a remarkable ability for formation of organizing centers, due to the spontaneous nature of identity acquisition, there is quite significant variability from organoid to organoid and between experiments. We also observed the formation of regions of non-forebrain identity. While we did not analyze those regions by marker staining, transcriptome profiling of individual

cerebral organoids has revealed transcriptional signatures of other brain regions such as hindbrain and spinal cord, and even other embryonic tissues such as digestive tract and skeletal system development (Lancaster *et al.*, 2016). This underlines the importance of careful marker stainings to recognize different tissue identities within 3D brain organoids. This is especially important for studies in which organoids with different genetic backgrounds are analyzed. We propose the use of FOXP1 staining as evidence for forebrain identity and within those tissues TBR2 staining in the SVZ as a marker for dorsal forebrain. The dependence on molecular markers published for *in vivo* studies where identity can be inferred from morphological landmarks is of course a limitation for further classification of regional identities within organoids. Currently, this can be overcome with combinatorial stainings to identify the region of interest. Further large-scale sequencing efforts such as Kerwin *et al.* (2010) and Fagerberg *et al.* (2014) will contribute to the identification of new region-specific molecular markers in the human developing brain that can be used in the organoid field.

Materials and Methods

Human embryonic stem cell culture

Human embryonic stem cells H9 [Wisconsin International Stem Cell (WISC) Bank, WiCell Research Institute, WA09 cells] were cultured according to WiCell protocols (<http://www.wicell.org/home/support/stem-cell-protocols/stem-cell-protocols.cmsx>) on MEF feeders (CF-1 MEF, irradiated, GlobalStem) in hESC medium with bFGF or on Matrigel (Corning, hESC-Qualified) in mTeSR1 (Stemcell Technologies).

Generation and analysis of cerebral organoids

Cerebral organoids were generated and processed for analysis as described in great detail in Lancaster and Knoblich (2014).

Organoids were fixed in 4% PFA for 45–60 min at room temperature, washed in PBS, and cryoprotected in 30% sucrose in PBS overnight at 4°C. Three to five organoids were embedded together in blocks of 7.5% gelatine and 10% sucrose in PB and frozen in –30 to –50°C isopentane. Organoids were cut to 20- μ m cryosections, and every tenth section was collected onto a slide to obtain 10 slides containing serial sections representing the whole organoid. Slides were dried and stored at –80°C (long-term storage) or –20°C (short-term storage).

Immunofluorescence stainings

Slides were thawed, dried, and rehydrated in PBS. Slides were incubated for 1 h in 150 μ l blocking/permeabilization solution (0.25% Triton X, 4% normal donkey serum in PBS) under parafilm. The sections were incubated overnight at room temperature with 100 μ l primary antibodies in blocking solution (0.1% Triton X, 4% normal donkey serum in PBS) under parafilm, washed 3 \times 15 min in PBS + 0.05% Triton X, and incubated for 2 h with 1:500 secondary antibodies (Life Technologies) in blocking solution. Nuclei were counterstained with 1 μ g/ml DAPI in PBS for 15 min, and the slides were washed in the dark 2 \times 15 min in PBS + 0.05% Triton X and

1 \times 15 min PBS and mounted with Dako fluorescence mounting medium. See Table 1 for information on antibodies and dilutions.

Slides were imaged with the Panoramic SCAN slide scanner (3DHISTECH Ltd.) to obtain a representation of the entire organoids in 200- μ m intervals. For analysis of more than three markers within the same tissue, or in case of antibody incompatibility, adjacent sections on a neighboring slide were stained and analyzed. Complete scanning of all samples by the Panoramic SCAN Slide scanner allowed for comprehensive analysis of many tissues, stained with a large variety of different antibodies.

Dorsal forebrain tissue as well as ventral forebrain, PSPB, hem, and choroid plexus (with a diameter > 400 μ m) was detected in organoids at all stages analyzed (30–70 days old). Over time, we observed an apparent increase in organoids positive for these regions. Most likely, however, this apparent increase is due to the loss and/or reduced growth of malformed or mispatterned organoids over time rather than being a true increase in those tissues. To make up for this bias, organoids from several stages were combined for this experiment.

Tissue clearing and imaging in 3D

Organoids were fixed in PFA and processed essentially as described in Murray *et al.* (2015).

Table 1. Antibodies used in the study.

Antigen	Raised in	Company	Cat. No.	Dilution
BMP6	Rabbit	Novus Biologicals	NBP1-19733	1:100
CTIP2	Rat	Abcam	ab18465	1:100
DLX2	Goat	Santa Cruz	sc-18140	1:100
FOXP1	Rabbit	Abcam	ab 18259	1:200
FZD9	Rabbit	Acris	SP4153P	1:200
GFAP	Rabbit	Abcam	ab7260	1:750
GLT1	Guinea pig	Millipore	AB1783	1:500
GSX2	Rabbit	Millipore	abn162	1:500
LMX1A	Rabbit	Life Technologies	PA5-34470	1:50
MAP2	Mouse	Millipore	MAB3418	1:500
NKX2.1/TTF-1	Mouse	Dako	3,575	1:50
NRP2	Goat	R&D	AF2215	1:40
O4	Mouse	R&D	MAB1326	1:500
Olig1	Mouse	Millipore	MAB5540	1:200
PAX6	Mouse	DSHB	Pax6-s	1:200
PROX1	Mouse	Millipore	MAB5654	1:200
Reelin	Mouse	Millipore	MAB5366	1:250
SATB2	Rabbit	Abcam	ab34735	1:100
TBR2 (EOMES)	Chicken	Millipore	AB15894	1:100
TBR2 (EOMES)	Rabbit	Abcam	ab23344	1:300
TTR	Sheep	Abd Serotec	ahp1837	1:100
VGAT	Rabbit	Synaptic systems	131,013	1:2,000

Sparse labeling by GFP electroporation

Cerebral organoids were electroporated as previously described (Lancaster *et al*, 2013) with an integrating construct encoding EGFP containing a farnesylation sequence to enable membrane targeting (pT2-CAG-fGFP). The CAG promoter was isolated from pCAG-GFP (a gift from Connie Cepko, Addgene plasmid #11150) and inserted into the pT2/HB transposon donor plasmid (a gift from Perry Hackett, Addgene plasmid #26557), which was also modified to allow the insertion of sequences using Gateway cloning. A farnesylation sequence was inserted directly after the GFP of the pENTREGFP2 plasmid (a gift from Nathan Lawson, Addgene plasmid #22450), and this was then cloned into the above pT2-CAG-pDest using Gateway cloning (Thermo Fisher). CAG-driven sleeping beauty transposase plasmid was generated by cloning SB100X (pCMV(CAT)T7-SB100 was a gift from Zsuzsanna Izsvak, Addgene plasmid #34879) into the pCAGEN plasmid (a gift from Connie Cepko, Addgene plasmid #11160). Electroporation was performed by injecting 80 ng/ μ l pT2-Cag-fGFP and 240 ng/ μ l pCAGEN-SB100X. Organoids were fixed 2 weeks later and analyzed as described below for immunohistochemical analysis.

In situ hybridizations

Probe preparation

Wnt2b was amplified by PCR from human fetal brain cDNA (Invitrogen). The PCR reaction was diluted 1:500, and nested PCR was performed in two separate reactions with the forward or reverse primer containing the T7 site, respectively (Table 2). The PCR products were gel-purified by the Qiagen Gel Extraction Kit, and > 300 ng was used for reverse transcription with T7 polymerase, DIG-dNTPs, and RNase inhibitor for 4 h at 37°C. The samples were then incubated for 10 min at 37°C with 1 μ l DNase I (RNase free), and RNA was precipitated with EtOH and NaOAc3 at -20°C for 2 h, pelleted for 20 min at 4°C, washed with 70% EtOH, dried, and resuspended in 50 μ l nuclease-free H₂O. Five microliter was used to check the probe, and the rest was mixed 1:1 with 100% deionized formamide and stored at -20°C until use.

Sample preparation and hybridization procedure

Organoids were fixed for 4 h at 4°C in 4% PFA and cryoprotected by sinking in 30% sucrose in PBS overnight at 4°C. They were embedded in OCT compound, frozen, and stored at -80°C. Organoids were sectioned to 20- μ m cryosections. All solutions up to

probe hybridization were RNase free. Slides were post-fixed for 15 min in 4% PFA at RT, washed in PBS, bleached for 15 min in 3% H₂O₂-PBS at RT, washed with PBS, and treated for 5 min at RT with 40 μ g/ml proteinase K. The slides were directly fixed with 4% PFA for 15 min, washed in PBS, and incubated for 10 min in fresh acetylation solution (250 ml H₂O, 2.235 ml triethanolamine, 0.437 ml HCl, 0.938 ml acetic anhydride). Slides were pre-hybridized with hybridization buffer (25 ml 20 \times SSC, 250 ml deionized formamide, 5 ml salmon sperm DNA, 10 ml 50 \times Denhart's solution, 205 ml H₂O, 5 ml 0.5 M EDTA) at 65°C for 3 h in a slide mailer and incubated overnight with *in situ* probe 1:400 (denatured for 10 min at 70°C and quickly cooled on ice) in hybridization buffer at 65°C. Slides were washed 1 \times 15 and 2 \times 30 min in fresh wash solution (1 \times SSC, 50% formamide, 0.1% Tween-20), 2 \times 30 min in 1 \times MABT (5 \times MABT: 58 g maleic acid, 43.8 g NaCl, ca. 38 g NaOH to pH 7.5, 50 ml 10% Tween-20, to 1 l with H₂O), blocked 2–3 h with 150 μ l blocking solution (1 \times MABT, 2 ml 10% blocking solution–blocking reagent Roche, 2 ml inactivated sheep serum, H₂O to 10 ml) under parafilm, and incubated with DIG AP FAB fragments 1:1,500 overnight at 4°C. The slides were washed 5 \times 20 min in 1 \times MABT, 2 \times 10 min in fresh staining solution (4 ml 5 M NaCl, 1 ml 1 M MgCl₂, 20 ml 1 M Tris pH 9.5, H₂O to 200 ml), and incubated with AP substrate (Roche) in the dark until signal appeared. Slides were washed in PBS, fixed 10 min in 4% PFA, washed, and mounted.

Expanded View for this article is available online.

Acknowledgements

We thank all members of the Knoblich, Lancaster, and Chung laboratories for discussions and support. We thank Raika Sieger for technical support. We are grateful to all IMP/IMBA and VBCF service facilities for providing technical support. We are particularly indebted to G. Petri and P. Pasierbek for imaging support and T. Lendl for help with 3D reconstructions. We thank Alex Phillips for generation of the membrane-targeted GFP construct. M.A.L. was funded by a Marie Curie Postdoctoral Fellowship. Work in M.A.L.'s laboratory is supported by the Medical Research Council MC_UP_1201/9. Work in J.A.K.'s laboratory is supported by the Austrian Academy of Sciences, the Austrian Science Fund (grants I_1281-B19 and Z_153_B09), and an advanced grant from the European Research Council (ERC). K.C. is supported by Burroughs Wellcome Fund Career Awards at the Scientific Interface, the Searle Scholars Program, Packard award in Science and Engineering, NARSAD Young Investigator Award, JPB Foundation (PIIF and PNDRF), NCSOFT Cultural Foundation, and NIH (1-U01-NS090473-01). Resources that may help enable general users to establish the SWITCH methodology are freely available online (<http://www.chunglabresources.com>).

Author contributions

MR, MAL, and JAK conceived the project. MR, MAL, SB, and AP performed the experiments. TK and HC performed organoid clearing and imaging under the supervision of KC. MR, MAL, SB, and JAK wrote the manuscript. JAK directed and supervised the project.

Conflict of interest

M.A.L. and J.A.K. are inventors on a patent application (WO2014/090993) describing the cerebral organoid method. K.C. is a cofounder of LifeCanvas Technologies, a start-up that aims to help the research community adopt technologies developed by the Chung Laboratory.

Table 2. Primer sequences to generate Wnt2b probe.

Pcr1 from cDNA	For	GACCGGGACCACACCGTCTTTGG
Pcr1 from cDNA	Rev	GGTGGAGGGTGGAGGAAGGTG
Nested PCR	For-T7	aaaataatcagactcactatagggagaCATG CTCAGAAGTAGCCGAGA
Nested PCR	Rev	ATGCAAGGATCTTGCTTTT
Nested PCR	For	CATGCTCAGAAGTAGCCGAGA
Nested PCR	Rev-T7	aaaataatcagactcactatagggagaATGC AAGGATCTTGCTTTT

References

- Abu-Khalil A, Fu L, Grove EA, Zecevic N, Geschwind DH (2004) Wnt genes define distinct boundaries in the developing human brain: implications for human forebrain patterning. *J Comp Neurol* 474: 276–288
- Borello U, Pierani A (2010) Patterning the cerebral cortex: traveling with morphogens. *Curr Opin Genet Dev* 20: 408–415
- Camp JG, Badsha F, Florio M, Kanton S, Gerber T, Wilsch-Bräuningner M, Lewitus E, Sykes A, Hevers W, Lancaster M, Knoblich JA, Lachmann R, Pääbo S, Huttner WB, Treutlein B (2015) Human cerebral organoids recapitulate gene expression programs of fetal neocortex development. *Proc Natl Acad Sci USA* 112: 15672–15677
- Caronia-Brown G, Yoshida M, Gulden F, Assimacopoulos S, Grove EA (2014) The cortical hem regulates the size and patterning of neocortex. *Development* 141: 2855–2865
- Chambers SM, Fasano CA, Papapetrou EP, Tomishima M, Sadelain M, Studer L (2009) Highly efficient neural conversion of human ES and iPS cells by dual inhibition of SMAD signaling. *Nat Biotechnol* 27: 275–280
- Chizhikov VV, Lindgren AG, Mishima Y, Roberts RW, Aldinger KA, Miesegaes GR, Currlle DS, Monuki ES, Millen KJ (2010) Lmx1a regulates fates and location of cells originating from the cerebellar rhombic lip and telencephalic cortical hem. *Proc Natl Acad Sci USA* 107: 10725–10730
- Eiraku M, Watanabe K, Matsuo-Takasaki M, Kawada M, Yonemura S, Matsumura M, Wataya T, Nishiyama A, Muguruma K, Sasai Y (2008) Self-organized formation of polarized cortical tissues from ESCs and its active manipulation by extrinsic signals. *Cell Stem Cell* 3: 519–532
- Elston GN (2003) Cortex, cognition and the cell: new insights into the pyramidal neuron and prefrontal function. *Cereb Cortex* 13: 1124–1138
- Englund C (2005) Pax6, Tbr2, and Tbr1 are expressed sequentially by radial glia, intermediate progenitor cells, and postmitotic neurons in developing neocortex. *J Neurosci* 25: 247–251
- Fagerberg L, Hallström BM, Oksvold P, Kampf C, Djureinovic D, Odeberg J, Habuka M, Tahmasebpoor S, Danielsson A, Edlund K, Asplund A, Sjostedt E, Lundberg E, Szilgyarto CAK, Skogs M, Takanen JO, Berling H, Tegel H, Mulder J, Nilsson P et al (2014) Analysis of the human tissue-specific expression by genome-wide integration of transcriptomics and antibody-based proteomics. *Mol Cell Proteomics* 13: 397–406
- Gaspard N, Bouschet T, Hourez R, Dimidschstein J, Naeije G, van den Aemele J, Espuny-Camacho I, Herpoel A, Passante L, Schiffmann SN, Gaillard A, Vanderhaeghen P (2008) An intrinsic mechanism of corticogenesis from embryonic stem cells. *Nature* 455: 351–357
- Geffers L, Herrmann B, Eichele G (2012) Web-based digital gene expression atlases for the mouse. *Mamm Genome* 23: 525–538
- Georgala PA, Carr CB, Price DJ (2011) The role of Pax6 in forebrain development. *Dev Neurobiol* 71: 690–709
- Geschwind DH, Rakic P (2013) Perspective. *Neuron* 80: 633–647
- Grove EA, Tole S, Limon J, Yip L, Ragsdale CW (1998) The hem of the embryonic cerebral cortex is defined by the expression of multiple Wnt genes and is compromised in Gli3-deficient mice. *Development* 125: 2315–2325
- Grove EA, Monuki ES (2013) Chapter 2 - Morphogens, patterning centers, and their mechanisms of action. In *Patterning and cell type specification in the developing CNS and PNS*, Rubenstein JLR, Rakic P (eds), pp 25–44. Oxford: Academic Press
- Hansen DV, Lui JH, Flandin P, Yoshikawa K, Rubenstein JL, Alvarez-Buylla A, Kriegstein AR (2013) Non-epithelial stem cells and cortical interneuron production in the human ganglionic eminences. *Nat Neurosci* 16: 1576–1587
- Hevner RF, Daza RAM, Rubenstein JLR, Stunnenberg H, Olavarria JF, Englund C (2003) Beyond laminar fate: toward a molecular classification of cortical projection/pyramidal neurons. *Dev Neurosci* 25: 139–151
- Kadoshima T, Sakaguchi H, Nakano T, Soen M, Ando S, Eiraku M, Sasai Y (2013) Self-organization of axial polarity, inside-out layer pattern, and species-specific progenitor dynamics in human ES cell-derived neocortex. *Proc Natl Acad Sci USA* 110: 20284–20289
- Kerwin J, Yang Y, Merchan P, Sarma S, Thompson J, Wang X, Sandoval J, Puellas L, Baldock R, Lindsay S (2010) The HUDSEN Atlas: a three-dimensional (3D) spatial framework for studying gene expression in the developing human brain. *J Anat* 217: 289–299
- Lancaster MA, Renner M, Martin C-A, Wenzel D, Bicknell LS, Hurles ME, Homfray T, Penninger JM, Jackson AP, Knoblich JA (2013) Cerebral organoids model human brain development and microcephaly. *Nature* 501: 373–379
- Lancaster MA, Knoblich JA (2014) Generation of cerebral organoids from human pluripotent stem cells. *Nat Protoc* 9: 2329–2340
- Lancaster MA, Corsini NS, Burkard TR, Knoblich JA (2016) Guided self-organization recapitulates tissue architecture in a bioengineered brain organoid model. *bioRxiv* doi:10.1101/049346
- Lui JH, Hansen DV, Kriegstein AR (2011) Development and evolution of the human neocortex. *Cell* 146: 18–36
- Ma T, Wang C, Wang L, Zhou X, Tian M, Zhang Q, Zhang Y, Li J, Liu Z, Cai Y, Liu F, You Y, Chen C, Campbell K, Song H, Ma L, Rubenstein JL, Yang Z (2013) Subcortical origins of human and monkey neocortical interneurons. *Nat Neurosci* 16: 1588–1597
- Mariani J, Simonini MV, Palejev D, Tomasini L, Coppola G, Szekely AM, Horvath TL, Vaccarino FM (2012) Modeling human cortical development *in vitro* using induced pluripotent stem cells. *Proc Natl Acad Sci USA* 109: 12770–12775
- Mariani J, Coppola G, Zhang P, Abyzov A, Provini L, Tomasini L, Amenduni M, Szekely A, Palejev D, Wilson M, Gerstein M, Grigorenko EL, Chawarska K, Pelphrey KA, Howe JR, Vaccarino FM (2015) FOXP1-dependent dysregulation of GABA/glutamate neuron differentiation in autism spectrum disorders. *Cell* 162: 375–390
- Medina L, Abellán A (2009) Development and evolution of the pallium. *Semin Cell Dev Biol* 20: 698–711
- Miller JA, Ding S-L, Sunkin SM, Smith KA, Ng L, Szafer A, Ebbert A, Riley ZL, Royall JJ, Aiona K, Arnold JM, Bennet C, Bertagnolli D, Brouner K, Butler S, Caldejon S, Carey A, Cuhaciyan C, Dalley RA, Dee N et al (2014) Transcriptional landscape of the prenatal human brain. *Nature* 508: 199–206
- Molyneaux BJ, Arlotta P, Menezes JRL, Macklis JD (2007) Neuronal subtype specification in the cerebral cortex. *Nat Rev Neurosci* 8: 427–437
- Murray E, Cho JH, Goodwin D, Ku T, Swaney J, Kim S-Y, Choi H, Park Y-G, Park J-Y, Hubbert A, McCue M, Vassallo S, Bakh N, Frosch MP, Wedeen Van J, Seung HS, Chung K (2015) Simple, scalable proteomic imaging for high-dimensional profiling of intact systems. *Cell* 163: 1500–1514
- O'Leary DDM, Chou S-J, Sahara S (2007) Area patterning of the mammalian cortex. *Neuron* 56: 252–269
- Paşca AM, Sloan SA, Clarke LE, Tian Y, Makinson CD, Huber N, Kim CH, Park J-Y, O'Rourke NA, Nguyen KD, Smith SJ, Huguenard JR, Geschwind DH, Barres BA, Paşca SP (2015) Functional cortical neurons and astrocytes from human pluripotent stem cells in 3D culture. *Nat Methods* 12: 671–678
- Qian X, Nguyen HN, Song MM, Hadiono C, Ogden SC, Hammack C, Yao B, Hamersky GR, Jacob F, Zhong C, Yoon K-J, Jeang W, Lin L, Li Y, Thakor J,

- Berg DA, Zhang C, Kang E, Chickering M, Nauen D et al (2016) Brain-region-specific organoids using mini- bioreactors for modeling ZIKV exposure. *Cell* 165: 1238–1254
- Rakic P (1974) Neurons in rhesus monkey visual cortex: systematic relation between time of origin and eventual disposition. *Science* 183: 425–427
- Sanes DH, Reh TA, Harris WA (2011) *Development of the nervous system*, 3rd edn. Waltham, MA: Academic Press.
- Sauvageot C (2002) Molecular mechanisms controlling cortical gliogenesis. *Curr Opin Neurobiol* 12: 244–249
- Shi Y, Kirwan P, Smith J, Robinson HPC, Livesey FJ (2012) Human cerebral cortex development from pluripotent stem cells to functional excitatory synapses. *Nat Neurosci* 15: 477–486
- Subramanian L, Remedios R, Shetty A, Tole S (2009) Signals from the edges: the cortical hem and antihem in telencephalic development. *Semin Cell Dev Biol* 20: 712–718
- Taverna E, Götz M, Huttner WB (2014) The cell biology of neurogenesis: toward an understanding of the development and evolution of the neocortex. *Annu Rev Cell Dev Biol* 30: 465–502